

Internal pressure in a low-rise building with existing envelope openings and sudden breaching

Amanuel S. Teclé¹, Girma T. Bitsuamlak^{*1} and Aly Mousaad ALY²

¹Laboratory for Wind Engineering Research, International Hurricane Research Center/Department of Civil and Environmental Engineering, Florida International University, Miami, Florida 33174, USA

²WindEEE Research Institute, Western University, London, ON, Canada

(Received October 4, 2010, Revised July 12, 2012, Accepted September 13, 2012)

Abstract. This paper presents a boundary-layer wind tunnel (BLWT) study on the effect of variable dominant openings on steady and transient responses of wind-induced internal pressure in a low-rise building. The paper presents a parametric study focusing on differences and similarities between transient and steady-state responses, the effects of size and locations of dominant openings and vent openings, and the effects of wind direction angle. In addition, the necessity of internal volume correction during sudden breaching was considered, i.e., a transient response experiment was investigated. A comparison of the BLWT data with ASCE 7-2010, as well as with limited large-scale data obtained at a 'Wall of Wind' facility, is presented.

Keywords: internal pressure; dominant openings; sudden breach; compartment; vents; gable roof; volume correction; boundary-layer wind tunnel; wall-of-wind

1. Introduction

Despite improvements in regulations and design provisions for buildings, the economic impact and loss of life as a result of wind induced-damage is still significantly high. Post-hurricane investigations have repeatedly reported that wind and wind-driven rain have been the cause of extensive damage to building components and their premises (FEMA 2005). The vulnerability to these meteorological events has been mainly attributed to the large suction external pressure that develops on the roof envelope of a building, especially at the corners, where wind-flow separation occurs. Internal pressure also contributes significantly to the uplift force generated when a door or window is left opened or broken due to either extreme pressure or the impact of wind-borne debris (Holmes 1979, Simiu and Scanlan 1996, Irwin and Sifton 1998). For low-rise buildings, wind-induced internal pressure can contribute greatly to the total design wind load, particularly in the presence of dominant openings (Holmes 1979, Stathopoulos *et al.* 1979, Holmes 2007). The algebraic sum of the external and internal pressures is used to assess the design wind loads on building envelope components, such as walls, roofs, roof tiles, windows and doors.

*Corresponding author, Associate Professor, E-mail: gbitsuam@UWO.ca

Even though the contribution of internal pressure to design wind-load is significant, few studies deal with internal aerodynamic and sudden breakage characteristics (Holmes 1979, Stathopoulos *et al.* 1979, Liu and Saathoff 1981,1982 Liu and Saathoff 1983, Vickery 1986, Vickery and Bloxham 1992, Sharma and Richards 1997, Sharma 2000, Guha *et al.* 2009) The internal pressure are affected in a complex manner by several factors, such as the shape of the building, the spatial variation of external pressure at the dominant opening, the geometries of the dominant openings, the size and location of dominant openings (i.e., with respect to the incoming wind flow direction, acute vs. obtuse angle) as well as the background porosity, ventilation openings, internal volume and compartmentalization (both vertical and horizontal), wind direction, upstream flow characteristics and flexibility of the building envelope (Holmes 1979, Stathopoulos *et al.* 1979, Liu and Saathoff 1981, Liu and Saathoff 1983, Vickery 1986, Sharma and Richards 1997). For buildings with a single dominant opening, the fluctuations of the internal pressure response closely correlates with the external pressure fluctuations that develop over the area of the dominant opening (Kopp *et al.* 2008). However, certain conditions of opening size and internal volume cause the formation of enough turbulence energy at the opening that, consequently, the internal pressure exceeds the external pressure fluctuation. This phenomena of excitation inside the building is called Helmholtz resonance (Holmes 1979, Oh *et al.* 2007, Kopp *et al.* 2008). The undamped natural frequency of the building cavity is referred to as the Helmholtz resonance frequency.

Most internal pressure studies have been carried out in boundary-layer wind tunnels (BLWT) at small scales. In BLWT studies, the large-scale building geometric length is scaled down by a certain ratio and the mean wind velocity and turbulence intensity profiles are replicated. With respect to the internal pressure analysis, a realistic assessment can be achieved only if one maintains the similarity of internal pressure dynamic characteristics between the large-scale and model-scale experiments (Holmes 1979). A non-dimensional analysis performed by Holmes (1979) showed that dynamic similarity can be ensured if the internal volume of the building is scaled correctly. The correct internal volume scaling is attained by multiplying the nominal volume obtained using length scale by the square of velocity scale ratio for cases where the ratio between full and wind tunnel velocities is not the same. It was also indicated that the effect of applying incorrect volume in the study of internal pressure fluctuations for low-rise buildings, such as residential and small industrial buildings with large-scale internal volumes less than 10000 m³, is less significant. Oh *et al.* (2007) reported that the background leakage worked to attenuate the internal pressure fluctuations induced through openings. For a building with envelope leakages and a single dominant opening, it was found that the Helmholtz resonance occurred and peak internal pressures were measured for wind direction normal to the wall having the dominant opening. A study by Kopp *et al.* (2008) examined the effects of dominant opening location and size, background leakage, compartmentalization of attic space from living space, the type of roof and vents. Their experiments showed that peak external roof pressures were negatively correlated in time with the internal pressures. It was also reported that decreasing the ratio of the internal volume to the opening area increased the peak internal pressures and Helmholtz resonance, particularly for wind directions normal to the opening.

Low-rise buildings, which are less well engineered compared to their high-rise counterparts, are more vulnerable to wind-induced damage. A single dominant opening could pose a critical failure to a building and this scenario is often used for wind load design purposes. During the passage of wind storms, potential scenarios for dominant openings include a door or window being left open

knowingly or unknowingly and significant internal pressure develops inside the building with time; or a closed door or window breach can be initiated by wind-borne debris to cause a transient response.

This could generate peak internal pressure that can lead to the bursting of leeward side doors/windows as well as the failure of roof components. Since openings covers are fixed to walls with non-structural frames, they are highly vulnerable to wind-borne missiles as tiny as small-size pebbles. Post-hurricane assessments have shown that most door and window breaches result from wind-borne debris, such as broken tile pieces, timber, stones, scrap metal, etc., that are removed from neighboring buildings. Even for cases where sudden building envelope breaching did not result in a major structural damage, it often creates a path for the intrusion of wind driven rain, which can cause damage to internal building components such as carpets, paint, electrical and sanitary facilities, dry walls and furniture. Water held in between these utilities commonly create a favorable environment for the formation of mold, rot and other health hazards. In some cases, houses become uninhabitable from mould infestation and odour. With respect to internal pressure, while the first scenario causes the formation of the steady-state condition, the second case may lead to an immediate internal pressure overshoot response that later transforms to the steady-state condition. The question with these two scenarios is whether the sudden overshoot due to the transient response is higher than the ensuing peak values of steady-state internal pressure response.

A BLWT study (Stathopoulos and Luchian 1989) to test the transient response of internal pressure in a building when a sudden opening occurs reported that the magnitude of transient response overshooting of internal pressure was lower than the subsequent steady-state peak fluctuations. The experimental study was carried out using a cubic box with a 0.152 m long side having no background leakage and the internal volume correction for velocity ratio was not applied. Similar results were reported in other experiments concluding that the transient internal pressure overshoot response would not be larger than the steady-state resonant response (Vickery and Bloxham 1992, Yeatts and Mehta 1992, Liu and Saathoff 1981, Sharma and Richards 1997, Guha *et al.* 2009). The sensitivity of sudden overshoot to dominant opening size and internal volume was also analytically studied in a multi-room building (Liu and Saathoff 1983). The study reported that the peak internal pressure resulting from sudden breach of dominant opening increases as the opening increases, and as the effective internal volume decreases.

On the other hand, other researchers (Sharma 2000 and Guha *et al.* 2009) have raised concerns over the conclusions reached above. The major concern raised was the possibility of synchrony between the formations of sudden opening with a peak gust when external pressure was at a peak. Based on their modelling, it was shown that the sudden overshoot response could be more significant compared to the subsequent peaks in the steady-state response, if the breaching occurred during a particularly strong gust. It is important to experimentally evaluate whether the transient overshoot could result in significant peak internal pressure values, thus indicating the need for an extensive study on the sudden breach of buildings.

A comparison of data from wind tunnel tests on low rise buildings with ASCE 7-2005 provisions by St. Pierre *et al.* (2005) reported that, generally, the ASCE 7-2005 standard code provisions underestimated the internal pressure response that results from fluctuating external pressure through dominant openings. The major factors that govern the wind-to-building interaction, such as geometry and location of the openings, orientation of the building, and proximity of adjacent buildings, are not perhaps realistically and comprehensively accounted for in the standard provisions (Simiu and Stathopoulos 1997, Whalen *et al.* 1998, Sharma and Richards 2003, Oh *et al.* 2007). Other studies also found that provisions for internal pressure were non-

conservative in current codes (Sharma and Richards 2003, 2005). The present study focuses on the characterization of internal pressure due to sudden door or window breaching, effects of volume corrections, varying dominant opening areas and their location with respect to the incoming (upstream) wind direction. It also compares aerodynamic data obtained from experiments carried out at small-scale (boundary-layer wind tunnel) and at large-scale Wall of Wind (WoW). The WoW is a 6-fan large-scale testing facility primarily used to study wind and wind-driven rain effects on low-rise structures (Chowdhury *et al.* 2009, Bitsuamlak *et al.* 2009, Aly *et al.* 2012). Recently, a new 12-fan version of the WoW is constructed (Aly *et al.* 2011). For comparison purposes, the WoW results presented in Tecele *et al.* (2012) are provided in the current study. The study also examines the peak internal pressure loading and compares with the wind load provisions of the ASCE 7-2010.

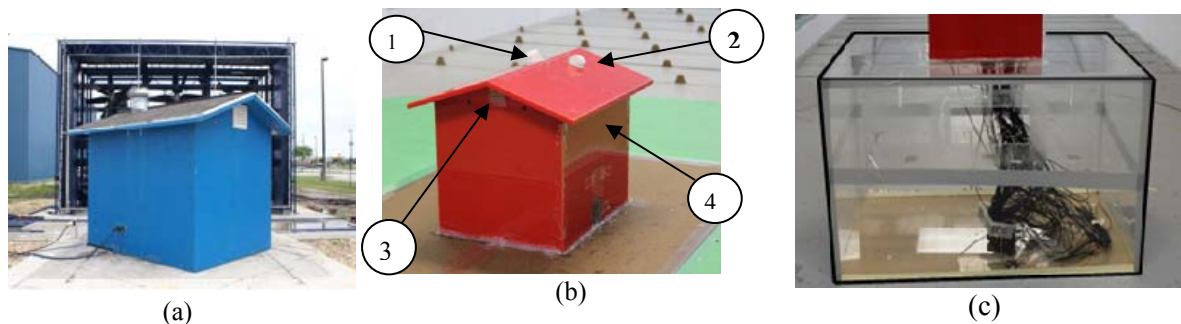


Fig. 1 Low-rise test building with gable roof at (a) large-scale at the Wall of Wind, (b) 1:9 small-scale at the BLWT, and (c) volume correction chamber before final placement under the BLWT floor. (1) Turbine vent; (2) goose neck vent; (3) gable end vent; (4) soffit vent.

2. Methodology

2.1 Boundary-layer wind tunnel setup

A gable roof low rise building with a 4:12 roof slope similar to a large-scale model used by Tecele *et al.* (2012) at the WoW, but constructed at a small-scale of 1:9 was studied at the RWDI Inc. boundary-layer wind tunnel (see Fig. 1). The geometry of the model building is shown in Fig. 2. For the sudden-breaching study, the small-scale test was more manageable and cost-effective. For comparison purposes, the large-scale building with all the details that might affect the overall external and internal flow dynamics, all the claddings, ventilation systems, and thickness of dominant openings, were properly scaled. For example, the small-scale model was constructed using acrylic sheets with a wall thickness scaled at 1:9. Mean wind velocity, turbulence intensity profiles as well as the spectra representing an open country exposure are shown in Fig. 3. The integral length is given in Fig. 3(d) as well. As can be seen from the figure, the integral length scale similitude is violated. This is the case in most low-rise residential building tests carried out in a standard wind tunnel, traditionally prepared for tall buildings. However, Holmes and Ginger (2012) showed that the internal pressure fluctuations are relatively insensitive to the parameter Φ_5 ($= L_u / A^{1/2}$) in which L_u is the integral length scale. In addition, the present study building is very

small (which is smaller than the integral length itself).

Accordingly, the correlation is higher (Fu *et al.* 2012). Thus, the length scale distortion is expected to have a limited effect on the present aerodynamic data. The power law index (α) and the turbulence intensity at mid-roof height (0.259 m from the ground) were 0.154 and 21%, respectively (Fig. 3). This is close enough to the target open terrain profile $\alpha = 0.16$ and a turbulence intensity of 20% at mid-roof height. The aerodynamic data was collected for a 90 s duration at a frequency of 512 Hz. The average mean wind speed at mean building roof height was 9.5 m/s.

Internal volume scaling: Providing proper internal volume distortion (correction) of a building model in a wind tunnel experiment is necessary in order to maintain the dynamic similarity of the internal pressure fluctuations between the wind tunnel and the large-scale model. For low rise buildings of large volume, the implementation of velocity and length scale helps maintain realistic internal pressure measurements, particularly the position of Helmholtz natural frequency relative to the turbulence spectrum. Holmes (1979) represented the dynamics of internal pressure response as a result of external pressure fluctuation through a dominant opening using the principles of the Helmholtz acoustic resonator. A dynamic equation, as shown in Eq. (1), was used where the first term in the equation represents the inertia of the mass of an air-slug passing through the opening, while the second term represents the non-linear damping that takes care of the energy losses through the dominant opening, and the third term represents the pneumatic resistance to the motion of the air-slug due to the cavity internal pressure, which is called stiffness.

$$\rho A l_e \ddot{X} + \frac{\rho A}{2k^2} \dot{X} \left| \dot{X} \right| + \frac{n P_o A^2}{V_o} X = \Delta P_e A \quad (1)$$

The following equation is obtained by rewriting Eq. (1) in terms of pressure coefficients.

$$\frac{\rho l_e V_o}{n A P_o} \ddot{C}_{pi} + \frac{\rho V_o^2 q}{2k^2 n^2 A^2 P_o^2} \dot{C}_{pi} \left| \dot{C}_{pi} \right| + C_{pi} = C_{pe} \quad (2)$$

At a constant atmospheric pressure and similar air density between large-scale and small-scale cases, the non-dimensional analysis of Eq. (2) results in Eqs. (3) and (4).

$$\frac{[\overline{U}^2 V_o]_m}{[\overline{U}^2 V_o]_f} = \frac{[A]_m^3}{[A]_f^3} x \frac{[P_o]_m}{[P_o]_f} x \frac{[\rho]_m}{[\rho]_f} \quad (3)$$

$$\frac{[V_o]_m}{[V_o]_f} = \frac{[L]_m}{[L]_f} x \frac{[\overline{U}]_f^2}{[\overline{U}]_m^2} \quad (4)$$

The undamped natural frequency (i.e., Helmholtz frequency) can be obtained from Eq. (2) and is given in Eq. (5).

$$f_{hh} = \frac{1}{2\pi} \sqrt{\frac{nAP_o}{\rho l_e V_o}} \quad (5)$$

where ρ is the density of air, A is the geometric area of the dominant opening, l_e is the characteristic length of the air slug, P_o is the ambient pressure of air, $P_e(t)$ is the external pressure driving the inertial force, C_{pi} and C_{pe} are internal and external pressure coefficients respectively, V_o is the effective volume of the cavity, L is the characteristic geometric length scale; \bar{u} is eave height wind speed, and subscripts m and f represent model and large-scale, respectively. For correct internal volume scaling and the appropriate measurement of the internal pressure fluctuations, the nominal volume obtained through length scaling needs to be magnified as given by Eq. (5). This could be done by providing an additional volume chamber underneath the wind tunnel turntable. In the present study, the model was prepared at a length scale of 1:9 and the test was conducted at a velocity scale of 1:4. Thus, the volume needed to be amplified by a factor of 16 as shown in Fig. 1(c). An airtight volume chamber box was attached to the base of the model building underneath the wind tunnel turntable, following the recommendation of Sharma *et al.* (2010).

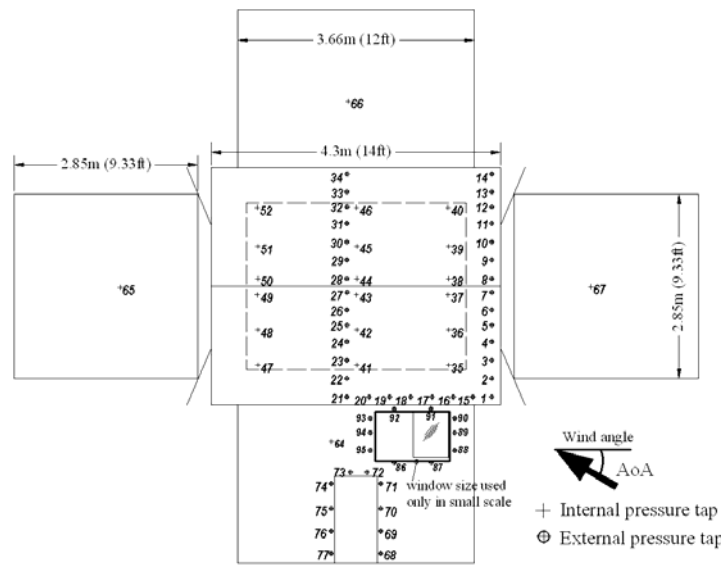


Fig. 2 Exploded view of building model with pressure tap layout and location of dominant openings.(Dimensions are given at large-scale)

Sudden door or window opening test setup: The mechanism implemented to create door/window sudden failure during the wind tunnel testing utilized a digital servo motor system shown in Fig. 4. In order to obtain consistent aerodynamic data, it was necessary to operate the door without interfering with the building's pressure taps. The best suited option for this application was the use of a remote controlled device. A radio control system normally used for model-aircraft was used as part of the electromechanical system and a radio transmitter was used to send out a signal of instructions (open/close the door), which were collected and interpreted by a radio receiver. The

receiver then translated these instructions to a servo motor, which carried out the instructions. The servo motor provided high operational speed necessary to simulate rapid failure of the door/window and substantial torque to hold the door/window closed against the wind-tunnel flow prior to opening. The completed servo motor time response is 0.1 s per 85° door turning.

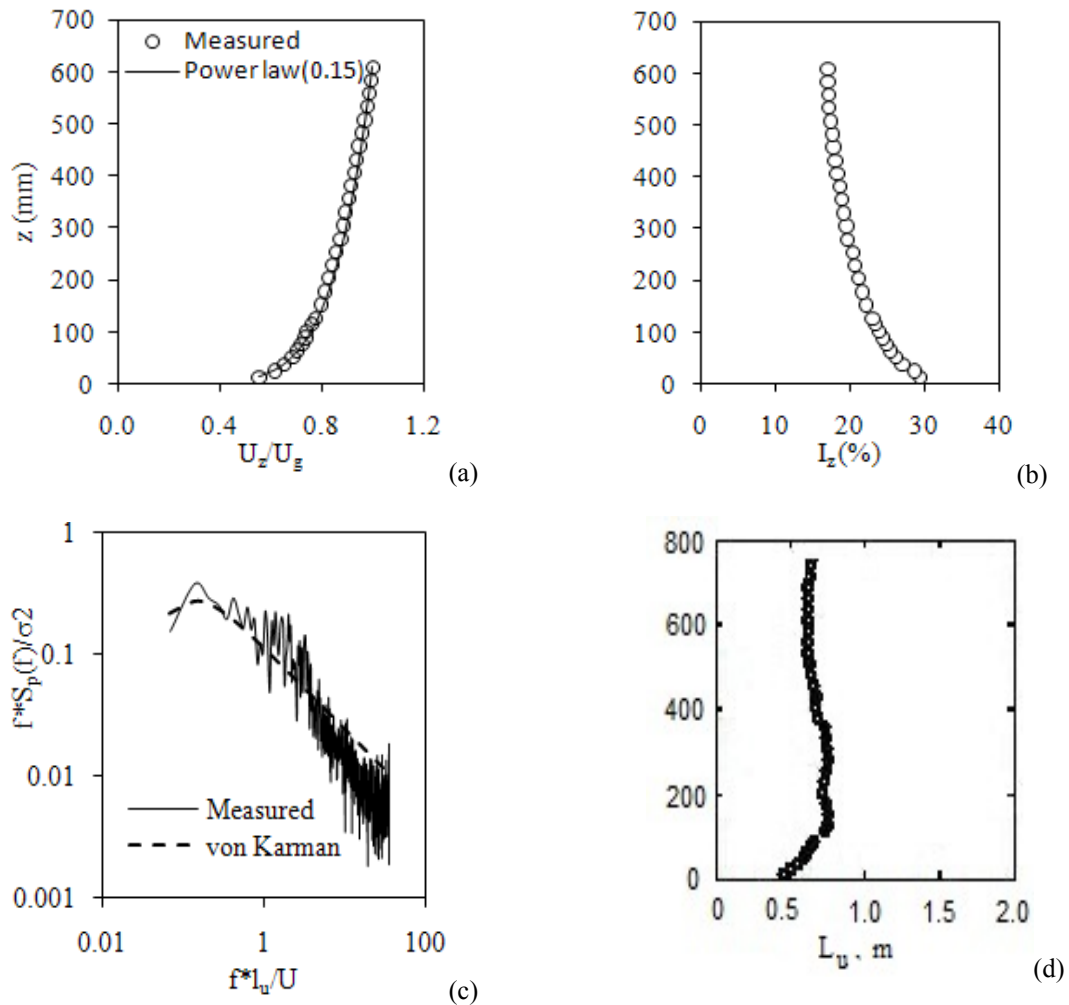


Fig. 3 BLWT flow characteristics (a) mean wind velocity profile, (b) turbulence intensity profile, (c) spectra and (d) integral length scale profile: f is the frequency, I_u is the turbulence intensity, L_u is the integral length scale, S_p is the power spectra, σ is the root mean square value of the along-wind velocity component (U)

Openings: The building has three doors and two windows. Inherent leakage due to cracks, joints and ducts was provided by incorporating uniformly distributed openings having circular holes (of diameter 1.6 mm). In all cases, the background leakage was 0.13% of the envelope surface area. Cross-ventilation of the attic space was provided through soffit openings, gable ends, ridges, goosenecks and turbine vents. Complete details are provided in Table 1.

Pressure tap layout: A total of 77 pressure taps were placed both externally and internally as shown in Fig. 2. Since the building has a partition wall at ceiling level (i.e., dividing the room into living space and attic), internal pressure taps were installed on the wall (one at the center of each wall), on the ceiling for the living room as well as on the roof sheathing for the attic room pressure measurements. A total of 18 pressure taps were distributed uniformly inside each room. As shown in Fig. 2 external pressure taps were installed on the edge and transverse centerline of the roof as well as eave to evaluate the pressure fluctuations at those representative locations of the roof envelope. To capture the external pressure fluctuations at the dominant openings, a total of ten pressure taps were placed around the periphery of each dominant opening. Measurements were obtained for a total of 21 wind angles of attack (AoA) in 10° increments (i.e., 19 AoA plus 45° and 135°). For symmetrical cases, tests were carried out only for 11 AoA's ranging between 0° and 90° . The 90° AoA coincides with the common normal of the wall containing the dominant opening.

Table 1 Dominant openings and background leakage distribution in small-scale dimensions

Description of opening	Dimensions (in)	Area (m^2/in^2)	Opening area ratio (%)	S*	Φ_5	
Windward wall	Door D1, (7.5%)	4.125×2	0.0053/8.25	7.5	2.26	10.3
	Door D2, (5%)	2.875×2	0.004/5.75	5.2	1.48	11.9
	Door D3, (3%)	1.0×3.3125	0.0021/3.31	3.0	0.56	16.4
	Window W1, (3.75%)	1.875×2.24	0.003/4.22	3.75	0.96	13.7
	Window W2, (9.0%)	3.78×2.52	0.006/9.53	9.0	2.72	9.7
Attic floor	Ceiling hatch	2×2.06	0.003/4.12	4	0.83	13.7
	Soffit screen (4 pcs)	1.6250.5	0.0021/3.25	3	0.49	16.4
	Gable end opening (2pcs)	1×1	0.0013/2	2	0.24	20.8
Roof	Ridge vent (2strips)	0.06×9.75	8E-5/0.117	0.11	0.00	83.9
	Turbine opening (dia. 1.1875")		1E-4/1.11	1.06	0.01	75.0
	Goose neck	0.44×1.06	3E-4/0.47	0.45	0.03	43.3

Experimental test cases:

Table 2 describes the various test scenarios performed to investigate internal and external pressures. Test cases 1 to 6 investigate the effects of the dominant opening sizes, while test cases 7 and 8 focused on transient internal pressure response during sudden openings of a door and a window, respectively. For test cases 7 and 8, the ceiling partition was removed so that the whole building acted as a single room (i.e., attic and living rooms were combined). Test cases 8a and 8b represent the same opening with and without volume correction, respectively, to assess the necessity of internal volume correction for transient response wind tunnel studies.

Internal and external pressure coefficient: First, the pressure data were corrected using a transfer function. The tubing transfer function approach used in this experiment was based on the

technique developed by Irwin *et al.* (1979) applicable for wall pressure measurements in wind engineering. Second, the time history pressure coefficients $P(t)$ of each pressure tap (both for external and internal) were used to compute the non-dimensional internal $C_{pi}(t)$ and external pressure $C_{pe}(t)$ coefficients by referencing the mean wind speed measured at mean roof height as given by Eqs. (6) and (7).

$$C_{pi} = \frac{P_{ij}(t)}{\frac{1}{2}\rho\bar{U}^2} \quad (6)$$

$$C_{pe} = \frac{P_{ej}(t)}{\frac{1}{2}\rho\bar{U}^2} \quad (7)$$

here P_{ij} and P_{ej} are the measured internal and external differential pressures, respectively, at the j^{th} tap (it is worth noting that the reference static pressure for wind tunnel tests was the tunnel static pressure where the dynamic pressure is not included). The reference static pressure for WoW testing is the atmospheric pressure measured at a point located far away from the wind field; ρ is air density; \bar{U} is the mean wind speed at mean roof height of the building. In the present study, unless otherwise mentioned, a mean hourly wind speed is used to obtain the pressure coefficients. The time scale is calculated from the following law of similitude: Time Scale = (geometric scale)/(velocity scale) = 9/4 = 2.25. Accordingly, a 1.5 minute wind tunnel period corresponds to 3.375 minutes at full scale. The corresponding mean hourly wind speed measured at the wind tunnel is obtained by applying a conversion factor of 1.15 (ASCE 7-2005). To remove the uncertainties inherent in the randomness of the peaks, probabilistic analyses were performed using the procedure developed by Sadek and Simiu (2002) for obtaining statistics of pressure peaks from observed pressure time histories. The method is stable and can predict peak values from short time records that correspond to longer time records.

3. Results and discussions

3.1 Internal pressure variation with respect to dominant openings

Fig. 5 describes the distribution of internal pressure with dominant openings (door- D_2 with 5% opening and window- W_1 with 3.75% opening) as well as background leakage (*blg*). The mean internal pressure coefficient C_{pi} due to only background leakage was uniform in distribution but very low in magnitude and no significant variation was observed with respect to wind direction. For Test Case 1a, with 0.13% background leakage and vent openings, the mean C_{pi} was -0.09. However, for background leakage with vent openings closed, the mean C_{pi} became positive ranging between 0.05-0.07. This shows that closing vent openings, such as soffit over the perimeter of the roof envelope, gable ends, and ridge vents, could initiate the buildup of positive pressure inside the attic room. For the dominant opening case, the smaller opening W_1 caused higher root mean square (*rms*) C_{pi} at AoA of 10°-80° compared to the larger opening D_2 . This is attributed to the W_1 proximity to the corner of the building.

The window W_1 and door D_2 are located 0.75 m and 1.8 m from the upstream wall corner, respectively. In addition, the window is located higher compared to the door. Similarly, irrespective of their size, the window with 3.75% opening exhibited a higher positive peak and suction internal pressure distribution than the door with 5% opening. The peak C_{pi} occurred at about 70° AoA, while the suction pressure occurs at 10° wind AoA. This demonstrated that, besides the size of the dominant openings, the location with respect to the upstream wall corners and the ground, and wind AoA are important parameters that affect the internal pressure.

According to Holmes (1979) and Kopp *et al.* (2008), when the ratio of the *rms* value of C_{pi} to that of C_{pe} is greater than one (i.e., $C_{pi}' / C_{pe}' > 1$), significant Helmholtz resonance is expected. In all of the wind AoA examined, the internal *rms* values are lower than the external *rms* values measured at the periphery of the respective dominant opening. This is believed to be due to the uniform nominal background leakage and the presence of the vents, which caused damping and hence reduction of the intensity of the internal pressure fluctuations. The trend of the peak C_{pi} and C_{pe} , however, illustrates good correlation between the internal pressure and the external pressure at the dominant opening. For example, the *rms* of the internal and external pressure coefficients for the two biggest dominant openings (i.e., $D_1=7.5\%$ and $W_2=9\%$), as shown in Fig. 6, did not indicate enough internal pressure excitation. In addition, spectral analysis of the internal pressure time history did not show any significant peak due to Helmholtz resonance (see Fig. 7).



Fig. 4 Sudden failure simulation technique: (a) digital servo motor Hitec HSG-5084MG (courtesy of ServoCity™) and (b) window assembly and servo in open position

To put the results in context, the parameters of the building studied are converted into a non-dimensional form. It has been shown (see Holmes and Ginger 2009, 2012) that for a single dominant opening, the ratio of r.m.s. internal pressure to the r.m.s. external pressure near the opening is a unique function of the non-dimensional parameters S^* and Φ_5 where $S^* = (a_s / \bar{U})^2 \cdot A^{3/2} / V$, in which a_s is the speed of sound (240 m/s) and $\phi_5 = L_u / A^{1/2}$. For example for the Door D1 case (7.5% area), S^* is approximately 2.26 and Φ_5 is 10.3. For those parameters Holmes and Ginger (2012, Fig. 3) showed that the ratio of $C'_{p,i}$ to $C'_{p,e}$ is about 1. This seems to agree with the results presented in the current study. The values of the non-dimensional parameter S^* and Φ_5 are given in Table 1.

Similar to the observation in Fig. 5, even though the window opening W_1 is smaller than the door openings D_1 and D_2 , the building experienced higher fluctuation in internal pressure due to W_1 as shown in Fig. 8. It is observed that the mean C_{pi} with the window openings was around $+0.9$ which is 50% higher than that due to the door openings. Also from Fig. 8(b), it can be seen that the r.m.s. C_{pi} for window openings (W_1 and W_2) is significantly higher than that with the door openings particularly for the wind AoA between 0° and 90° . Both windows are located higher and off-center close to a corner region where higher turbulence due to flow separation is anticipated, particularly for wind flow parallel to the windows. This has a direct influence on the dynamics of the internal pressure.

Table 2 Summary of test cases for low-rise building with gable and hip roof

Description	Test cases	Dominant openings	Inherent leakage	Ceiling window	Vents: ridge/soffit	Volume correction
Background leakage (big) combination	Test 1a	-	√	-	√	√
	Test 1b	-	√	-	-	√
	Test 1c	-	√	√	-	√
7.5% Door opening combination	Test 2a	D_1	√	-	-	√
	Test 2b	D_1	√	√	-	√
	Test 2c	D_1	√	√	√	√
	Test 2d	D_1	√	-	√	√
5% Door opening combination	Test 3a	D_2	√	-	-	√
	Test 3b	D_2	√	√	-	√
	Test 3c	D_2	√	√	√	√
	Test 3d	D_2	√	-	√	√
3% Door opening	Test 4d	D_3	√	-	√	√
3.75% Window opening combination	Test 5a	W_1	√	-	-	√
	Test 5b	W_1	√	√	-	√
	Test 5c	W_1	√	√	√	√
	Test 5d	W_1	√	-	√	√
9.0% Window opening combination	Test 6a	W_2	√	-	-	√
	Test 6b	W_2	√	√	-	√
	Test 6c	W_2	√	√	√	√
	Test 6d	W_2	√	-	√	√
Sudden breakage of door and window						
7.5% Door opening	Test 7a	D_1	√	-	-	√
9.0% Window opening	Test 8a	W_2	√	-	-	√
	Test 8b	W_2	√	-	-	-

As a result, the peak internal pressure coefficient due to the open windows and doors occurred at different wind AoA. Between 10° and 50° wind AoA, both window openings exhibited fairly

similar internal pressure variation regardless of the opening size (3.75% vs 9%). The distance between the upstream wall corner and the dominant opening has a significant impact on the r.m.s. values. For shorter distance between the windward wall corner and window opening, the r.m.s. fluctuation is considerably higher than the case when this distance is larger. For example, the r.m.s. for the 9% window (W_2) at 30° wind AoA is 0.36; however, at 150° AoA the r.m.s. value is 0.1. A similar trend was observed for 20° and 160° AoAs.

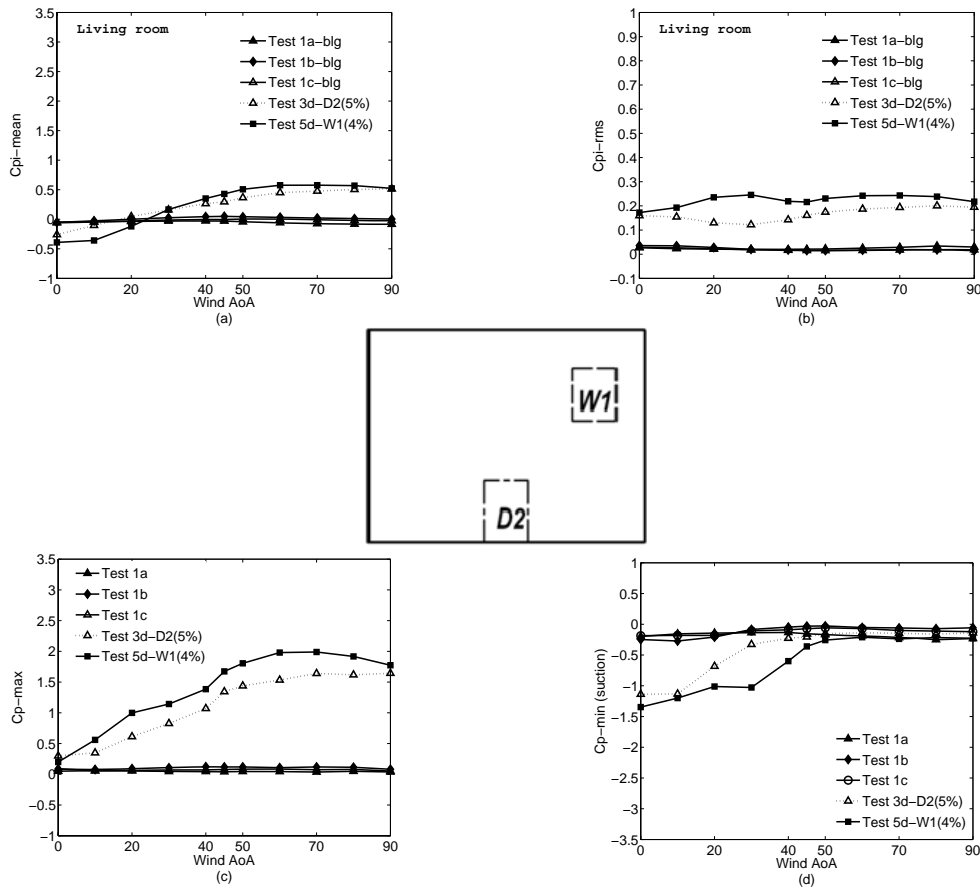


Fig. 5 Internal pressure comparison between background leakage (*blg*), 5% opening door and 4% opening window

Fig. 8(c) shows the internal pressure coefficients due to window openings reaching a peak value at $70\text{--}75^\circ$ wind AoA, whereas in the case of door openings, the maximum peak value occurs at 100° wind AoA. For wind AoA above 90° , the location of the window opening is far from the left corner (where upstream flow occurs) as compared to that of the door opening, which is located at the center of the wall. Consequently, the magnitude of the internal pressure due to both window openings is lower than that due to the door openings regardless of its smaller size. It can be

concluded that the dominant openings located outside of the center region of the wall exhibit larger internal pressure for an obtuse wind AoA. For example, for wind AoA between 0° and 70° , the window W_1 with 4% opening generates larger internal pressure than that due to doors D_1 (7.5%) and D_2 (5%). On the other hand, for wind AoA between 100° and 180° , the door openings D_1 and D_2 generate higher internal pressure compared to windows W_1 and W_2 . This attests to the significance of the dominant opening location.

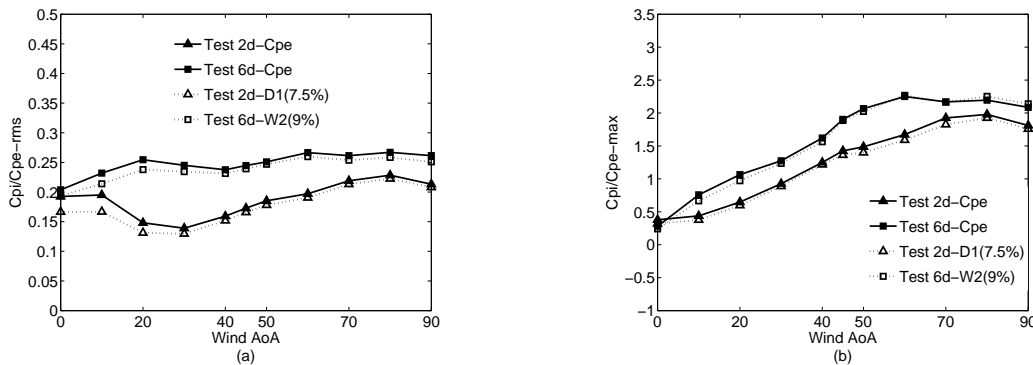
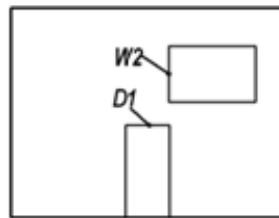


Fig. 6 Relationship of (a) *rms* and (b) maximum external pressure at dominant opening periphery vs internal pressure

3.1 The effect of ventilation openings

In this study, the closing and opening of different types of vent systems commonly used in residential buildings was investigated to examine their effect on the internal pressure inside the attic room. The attic hatch was left open along with door D_1 , and windows W_1 or W_2 . The vent openings include soffits around the perimeter of the roof, ridge, gable-end, goose neck and turbine vents.

Fig. 9 illustrates the distribution of mean and maximum attic internal pressure coefficients for closed and open vent opening cases (i.e., Test Cases 2b, 5b and 6b- the vents were closed, while for 2c, 5c and 6c- the vents were opened). For Test Case 2b (i.e., open door D_1), it was observed that the mean and peak attic internal pressures for the closed vent case were 40-45% larger compared to the open vent case. Similarly, for test cases 5 and 6, the mean and peak attic internal pressures were 90-140% larger for the closed vent compared to the open case.

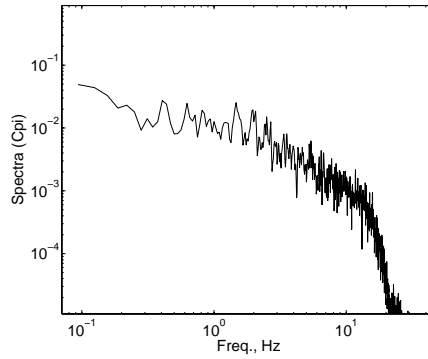


Fig. 7 Internal pressure spectra for sudden opening, (there is no significant Helmholtz resonance)

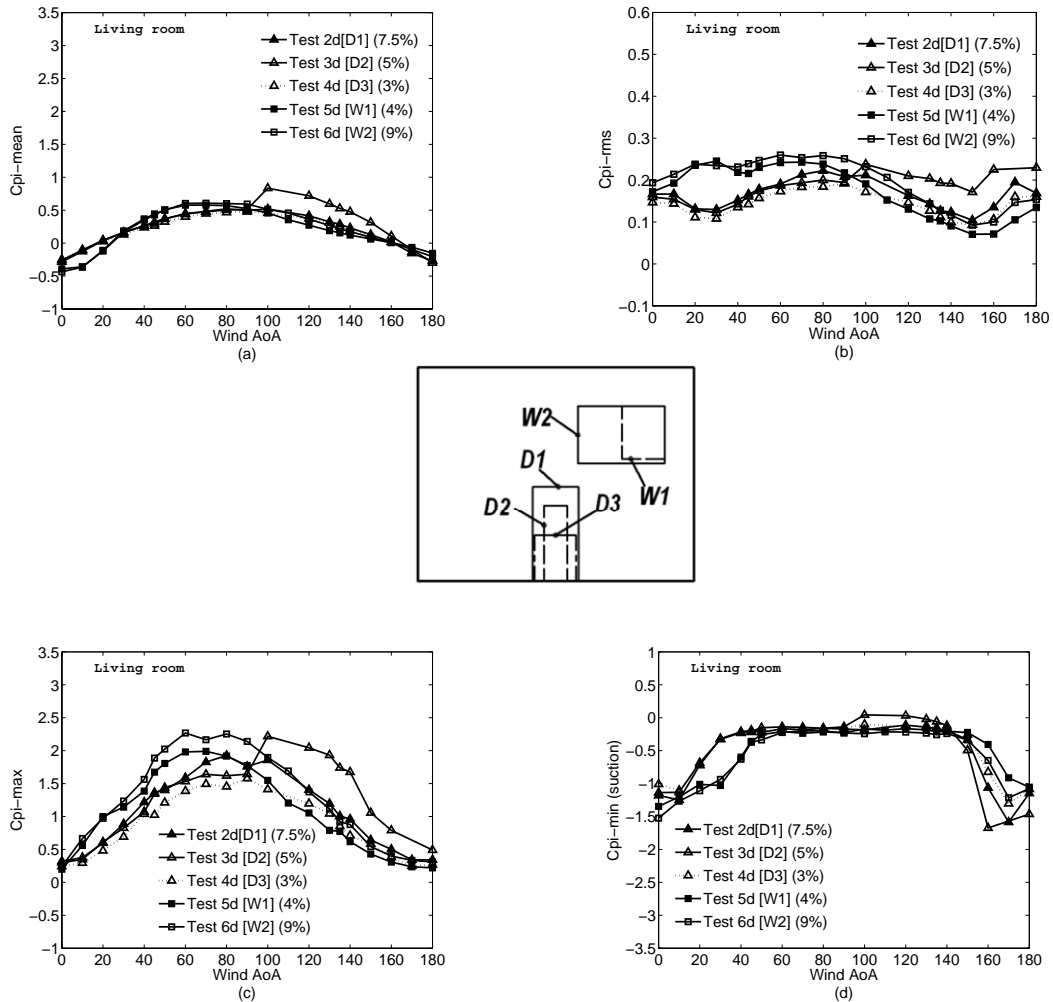


Fig. 8 Living room internal pressure (mean, rms, max and min) distribution due to various dominant openings

This clearly demonstrates that vent openings have a significant impact on the internal pressure of the attic. Closing the roof vent openings could aggravate the attic internal pressure.

The effect of vent openings on internal pressure inside the living room in the presence of dominant openings *D1*, *W1* and *W2* was also examined while the hatch was closed. The only interaction between the two spaces was through the uniform background leakage. Fig. 10 shows internal pressure inside the living room when the vent openings in the attic were opened and closed. As can be seen from the figure, the mean internal pressure inside the living room while the vent openings were closed, for both the door and window opening, was found to be 40-50% higher than that when the vents were left open.

Similarly the peak values of living room internal pressure were 20-25% higher for the closed vent case compared to the opened case. This re-affirms that the ventilation openings have considerable effect not only on pressures in the space where they are directly installed (i.e., the attic in this case), but also on internal pressure in the space that does not have direct interaction, such as the living room.

This indicates that vent operation could be useful not only for ventilation optimization, but also for prevention of wind driven rain intrusion, and regulation of the internal pressure.

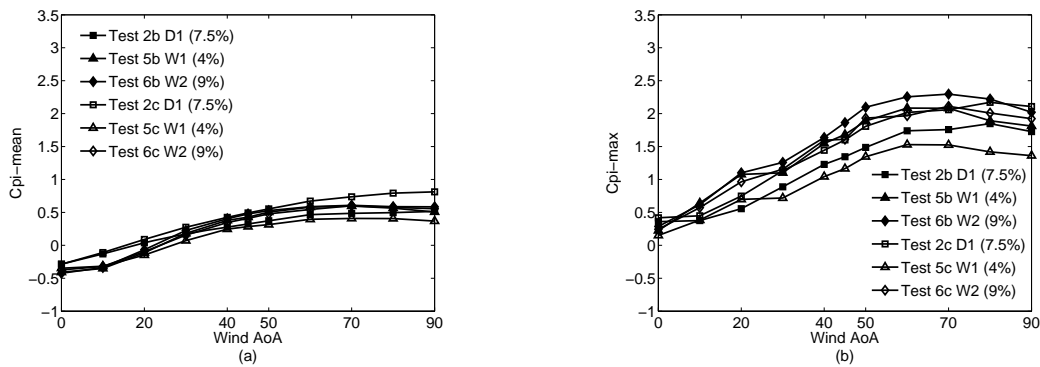


Fig.9 Comparison of internal pressure coefficient inside attic for an opened and closed vent (a) mean and (b) maximum

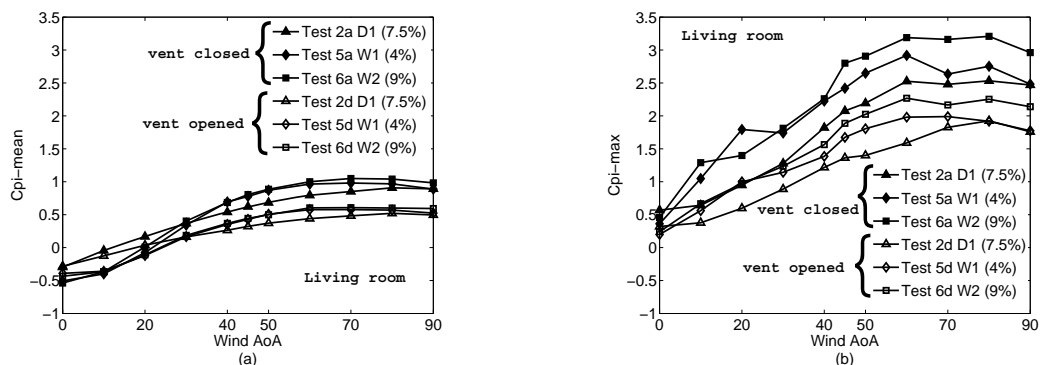


Fig. 10 Comparison of internal pressure inside living room for an opened and closed vent: (a) mean and (b) maximum

3.3 Sudden breach

The experimental study on the transient response of wind induced internal pressure to sudden breaching was carried out with the 7.5% (Test 7a) and 9% (Test 8a) dominant door opening located at the center and window opening located off-center with volume correction, respectively. Additional tests were also performed (i.e., Test 8b) without internal volume correction to examine the sensitivity of the transient response to the internal volume correction. All these tests were conducted for 45° , 75° and 90° wind AoA.

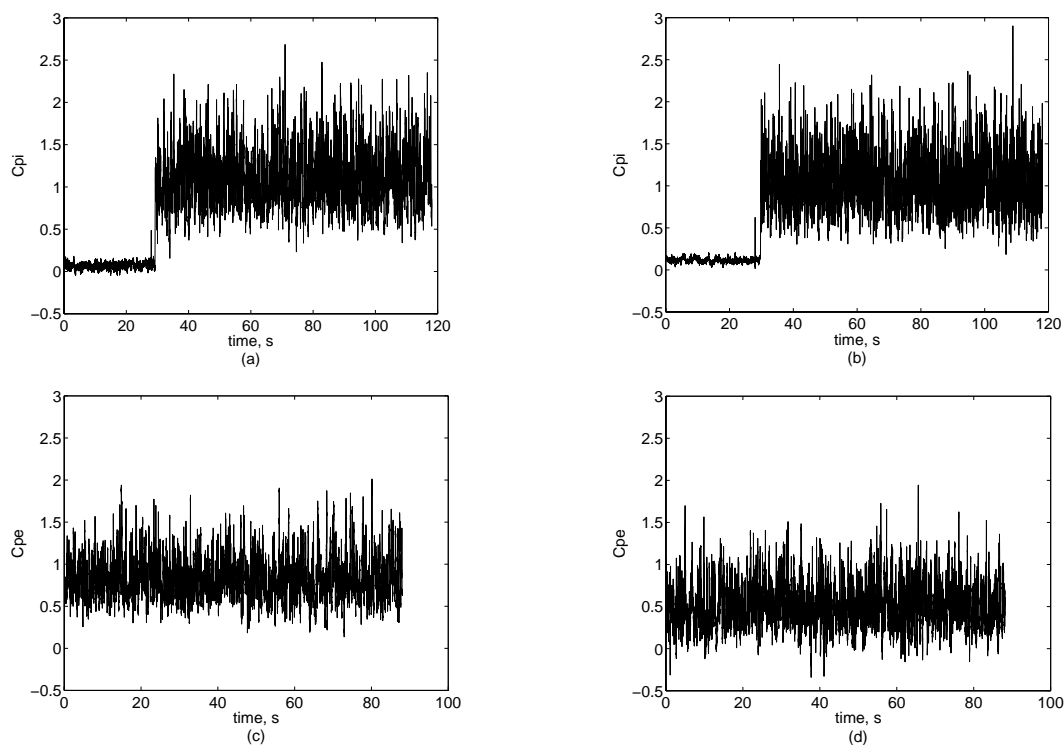


Fig. 11 Internal pressure coefficient time history for sudden breach of 7.5% door (a) and 9% window (b), and the corresponding external pressure coefficient on the periphery of 7.5% door (c), and 9% window (d)

A set of representative time histories showing the dynamic response of internal pressure is given in Fig. 11 for 75° wind AoA. The response can be divided into three regions: *Region 1*: time before sudden breach (i.e., $0 < t < 30$ s), *Region 2*: time during the sudden breach ($30 < t < 31$ s) and *Region 3*: time after the sudden breach ($31 < t < 120$ s). Based on repeated tests, it was observed that the building experiences a minimal internal pressure coefficient in the range of 0.15 before the sudden opening (i.e., *Region 1*). This internal pressure is due to a uniformly distributed background leakage. As the dominant opening is created during sudden breaching, the internal pressure increased from a mean value of 0.15 to a mean value of 1.2 for Test 7a, and 1.4 for Test 8a. Since

the flow is turbulent, the peak internal pressure response does not decay with time [see Fig. 11(a) and (b)] as expected for laminar flow where the peak dies out to the mean value with time. This phenomenon also verifies that the external pressure variations are consistently reflected in the internal pressure fluctuations consistent with observations in other studies (e.g., Stathopoulos and Luchian 1989). Comparing the variation of the internal pressure coefficient during and after the sudden breaching, there was a consistent trend that the transient response overshooting was lower than the steady-state peak values (for the 0.1 sec breaching time considered in the present study). It is worth noting that, due to the limited time response of the opening mechanism, the inability to control the synchrony in the experiments may be a reason why significant overshooting neither has been expected, nor was observed. In addition, the Helmholtz resonance was not evident from the spectra of the internal pressure under sudden door openings as shown earlier in Fig. 7.

Table 3 Response time comparisons

Test description	AoA	C_{pi} overshoot	$t(s)$
Test 7a	45	0.44	0.09
	75	1.23	0.09
	90	1.16	0.09
Test 8a	45	1.60	0.08
	75	1.56	0.07
	90	1.17	0.08
Test 8b	45	0.67	0.02
	75	1.38	0.05
	90	0.51	0.02

As described in Table 3 the response time for Test 7a (7.5% door opening, located at the center of the windward wall) was 0.09s for the three wind AoAs considered. Test 8a (9% window opening located close to the right side of the windward wall) was 0.08s at 45° and 90° wind AoA while 0.07s for 75° wind AoA. This reveals that the response time of transient internal pressure overshooting is comparatively faster for a larger dominant opening as the opening area (A) governs the resonance frequency (Eq. (3)) for a given internal volume (V). Comparing the response time with and without internal volume correction, Test 8b for the building with no volume correction exhibited 4 times faster response than that of Test 8a (i.e., 0.03s vs 0.08s) irrespective of their similar opening size. This underlines the necessity for volume correction for transient response experiments in a BLWT with velocity ratios other than unity. The distribution of the peak internal pressure after sudden breach is shown in Fig. 12 for tests 7a and 8a. The data points starting from the time the door or window opened were taken by computing the peak values. The peak internal pressure is fairly uniform across the building cavity for all tests undertaken.

3.4 Boundary-layer wind tunnel and WoW internal pressure comparison

Large-scale assessment of external and internal pressure commonly provide realistic data that reflects the actual aerodynamic phenomena tested on real-world building components, background leakage, effective internal volume and other factors that govern the internal flow dynamics such as inertia and viscous forces. It can reduce the uncertainties that are involved in the flow simulation

such as Reynolds number (Re) mismatch, characteristic length of the air-slug and Helmholtz frequency when using small-scale BLWT. However, the assessment of wind induced flow interaction using large-scale building is costly and time consuming.

The internal pressure distributions obtained from the model scale and large-scale (Tecele *et al.* 2012) building tests were compared for representative cases. It is to be recalled the present small-scale wind tunnel test building is a 1:9 scale of the large-scale building tested at the WoW. The comparison for dominant door D_1 with 7.5% opening and window W_1 with 3% opening were made. Fig. 13(a) and (c) show the comparison between the large- and small-scale gable building peak internal pressure coefficients inside the living room for a nominal background leakage as well as for a 7.5% door opening. Fig. 13(b) and (d) shows the same but for window opening. Considering the differences in the flow (for the WoW, an average alpha of 0.27 and turbulence intensity of 25% at mean roof height were used compared to the open terrain profile used at the BLWTL in the present study), the type of model (for instance large-scale incorporated actual construction materials), it can be inferred from the figure that there is a similar trend between the two scales. In both cases, peak positive internal pressure was noticed at about 70° - 75° wind AoA instead of the usual 90° . The r.m.s. internal pressure values of the large-scale building exhibited slight deviation from that of the small-scale wind tunnel data particularly for 0° to 50° wind AoA. This could be attributed to the higher turbulence used at the WoW.

3.5 Boundary-layer wind tunnel and ASCE 7-2010 internal pressure comparison

Wind tunnel data obtained for different opening sizes and wind AoA were converted into values referenced to a 3-second gust to correspond to the current wind load provisions, ASCE 7-2010. The comparisons are shown in Table 4. Only peak positive values at critical wind AoA are considered as this will have a significant effect on the net uplift force on the building roof envelope from wind design perspective. ASCE 7-2010 provides $GC_{pi} = \pm 0.55$ for partially enclosed buildings and $GC_{pi} = \pm 0.18$ for enclosed buildings. In the present work, the building with the various dominant openings coupled with the background leakage are in line with the definition of partially enclosed building while the building with only inherent background leakage represents

the enclosed case. For enclosed case, the experimental study was observed to be similar to the code, while for the dominant doors and window openings the present wind data consistently exceeded the values based on ASCE 7-2010, in most cases by a factor of two or greater. The building with the largest dominant openings experience the biggest difference, and this shows that the peak internal pressure values are not constant values as it consistently varies with respect to wind AoA, opening size and volume of the building.

4. Conclusions

The work described in this paper has investigated the steady and transient response of wind induced internal pressure for a low-rise building. Variable configurations of existing dominant and vent openings, background leakage and internal compartmentalization, as well as sudden breaching were studied in a standard boundary-layer wind tunnel. Wind-tunnel data were compared with corresponding large-scale WoW data, and ASCE 7-2010 values for components and cladding. The conclusions drawn are as follows:

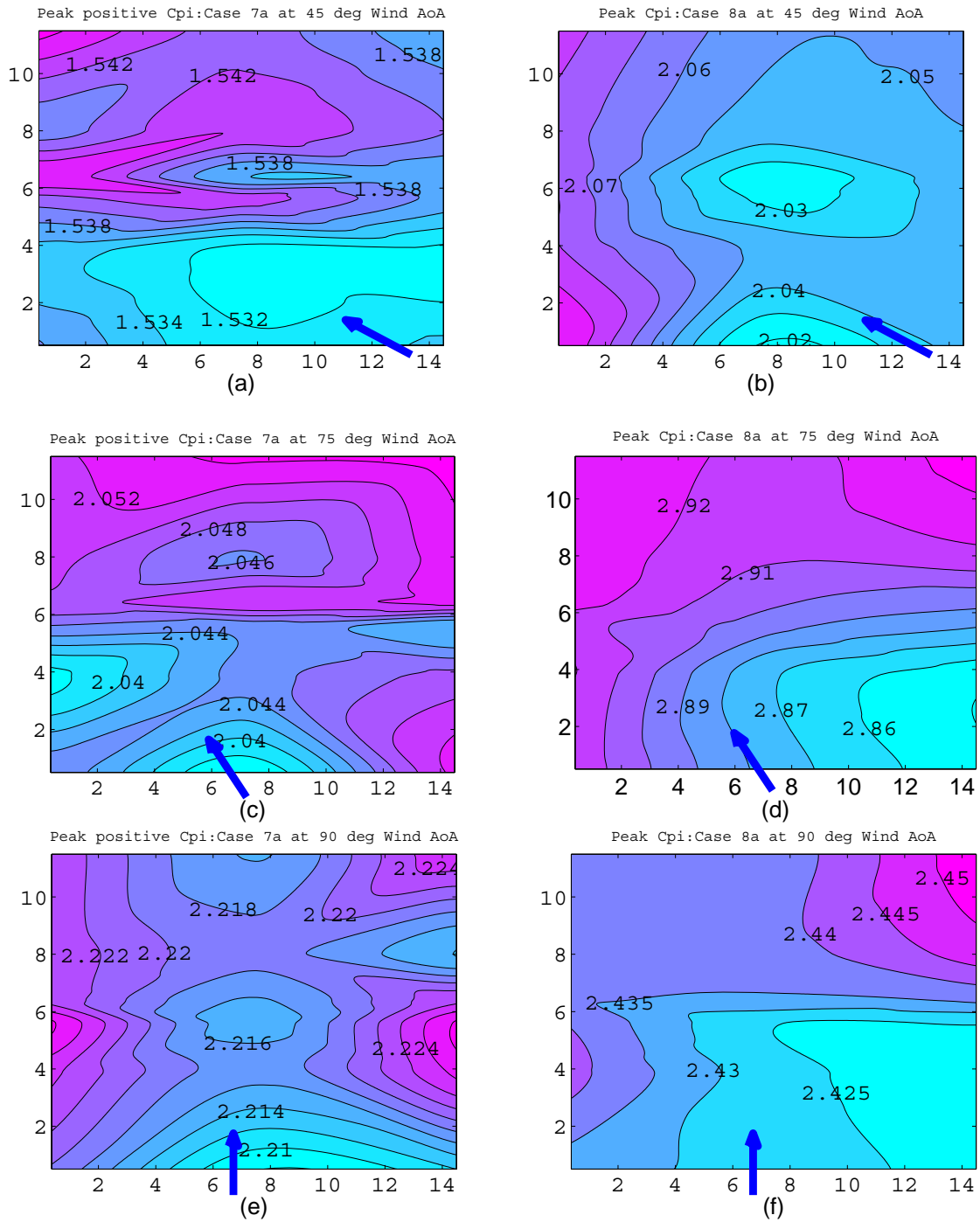


Fig. 12 Uniformity of internal pressure distribution at various wind AoA (45°, 75° and 90°)

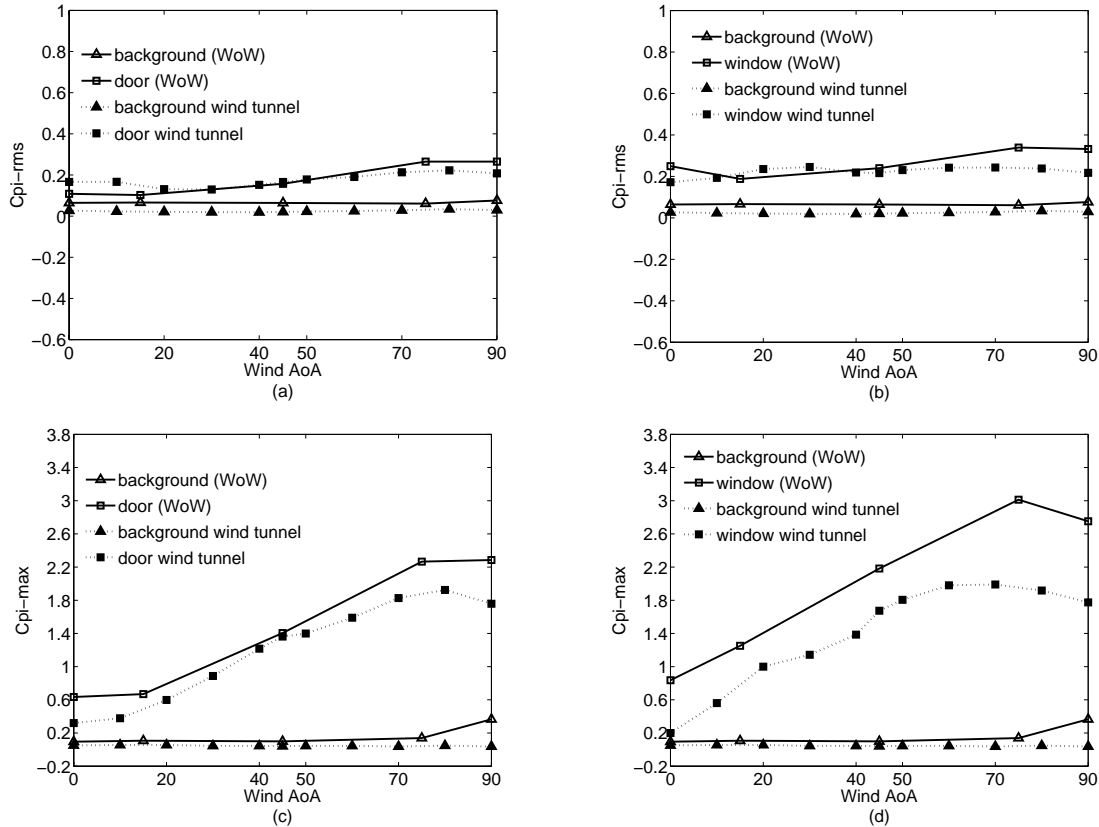


Fig. 13 Large-scale (WoW) to small-scale (BLWT) comparison of internal pressure: (a) and (c) for door opening (3%) and (b) and (d) for opening (7.5%)

1. Commonly ventilation openings are closed during wind storms, but this initiates the buildup of positive internal pressure inside the attic room. For a building having an all-round roof ventilation system, the mean and peak internal pressure underneath the roof sheathing can be 40-140% higher for a building with closed vents compared to the all-round open vent case.
2. In addition to the size of dominant openings, their location with respect to incoming wind direction affects the internal pressure. An opening located off-center exhibits higher positive peak and suction C_{pi} than its equivalent dominant opening located at the center wall. For the study case, the effect of the location of the dominant opening with respect to the incoming wind direction on the critical loading was higher than the opening size effect.
3. The transient overshooting response was found to be lower than the subsequent steady-state peak C_{pi} consistently for all wind directions, opening sizes and opening rate examined.
4. Correct internal volume scaling in BLWT was found necessary for the sudden opening case. A case without internal volume correction experiences a response time 4 times faster and 30-40% lower peak and mean C_{pi} than the building with volume correction.
5. The comparison between the large-scale and BLWT internal pressure responses shows good agreement in both the peak and mean values investigated by ASCE 7-2010 significantly

underestimates the peak positive internal pressure in all the configurations with dominant openings and building types considered while it produces similar values for background leakage cases.

Acknowledgments

This research was partly supported by the *National Science Foundation* under Grant No. 0846811, *IHRC's Florida Center of Excellence (FIU)* and *Western University start-up* grants. Any opinions, findings, and conclusions or recommendations expressed in this material are those of the authors and do not necessarily reflect the views of the granting agencies.

References

- Aly, A.M., Gan Chowdhury, A. and Bitsuamlak, G. (2011), "Wind profile management and blockage assessment for a new 12-fan Wall of Wind facility at FIU", *Wind Struct.*, **14**(4), 285-300.
- Aly, A.M., Bitsuamlak, G. and Gan Chowdhury, A. (2012), "Full-scale aerodynamic testing of a loose concrete roof paver system", *Eng. Struct.*, **44**, 260-270.
- ASCE 7-2005, (2006), *Minimum Design Loads for Buildings and Other Structures*, ASCE Standard, SEI/ASCE 7-05. American Society of Civil Engineers.
- ASCE 7-2010, (2010), *Minimum Design Loads for Buildings and Other Structures*, ASCE Standard, SEI/ASCE 7-10. American Society of Civil Engineers.
- Bitsuamlak, G.T., Gan Chowdhury, A. and Sambare, D. (2009), "Application of a full-scale testing facility for assessing wind-driven-rain intrusion", *Build. Environ.*, **44**(12), 2430-2441.
- Gan Chowdhury, A., Simiu, E. and Leatherman, S.P. (2009), "Destructive testing under simulated hurricane effects to promote hazard mitigation", *Nat. Hazards*, **10**(1), 1-10.
- FEMA, (2005), *Summary Report on Building Performance 2004 Hurricane Season*, FEMA 490, March 2005.
- Fu, T.C., Aly, A.M., Gan Chowdhury, A., Bitsuamlak, G.T., Yeo, D.H. and Simiu, E. (2012), "A proposed technique for determining aerodynamic pressures on residential homes", *Wind Struct.*, **15**(1), 27-41.
- Guha, T.K., Sharma, R.N. and Richards, P.J. (2009), "Analytical and CFD modeling of transient internal pressure response following a sudden opening in building/cylindrical cavities", *Proceedings of the 11th Americas Conference of Wind Engineering*, San Juan, Puerto Rico, June.
- Holmes, J.D. (1979), "Mean and fluctuating internal pressures induced by wind", *Proceedings of the 5th International Conference on Wind Engineering*, Colorado, USA, July.
- Holmes, J.D. (2007), *Wind Loading of Structures*, 2nd Ed., Taylor and Francis, London.
- Holmes, J.D. and Ginger, J.D. (2012), "Internal pressures- the dominant windward opening case – a review", *J. Wind Eng. Ind. Aerod.*, **100**(1), 70-76.
- Holmes, J.D. (2009), "Discussion of: net pressures on the roof of a low-rise building with wall opening", (Eds. R.N. Sharma and P.J. Richards), *J. Wind Eng. Ind. Aerod.*, **97**, 320-321.
- Irwin, H.P.A.H., Cooper, K.R. and Girard, R. (1979), "Correction of distortion effects caused by tubing systems in measurements of fluctuating pressures", *J. Wind Eng. Ind. Aerod.*, **5**(1-2) 93-107
- Irwin, P.A. and Sifton, V.L. (1998), "Risk Considerations for Internal Pressures", *J. Wind Eng. Ind. Aerod.*, **77-78**, 715-723.
- Kopp, G.A., Oh, J.H. and Incelet, R.D. (2008), "Wind-induced Internal Pressures in Houses", *J. Struct. Eng. -ASCE*, **134**(7), 1129-1138.
- Liu, H. and Saathoff, P.J. (1981), "Building internal pressure: sudden change", *J. Eng. Mech. - ASCE*, **107**(2), 309-321.

- Liu, H. and Saathoff, P. (1982), "Internal pressure and building safety", *J. Eng. Mech.- ASCE*, **108**(ST10), 2223-2234.
- Liu, H. and Saathoff, P.J. (1983), "Internal pressure of multi-room buildings", *J. Eng. Mech.- ASCE*, **109**(EM3), 908-919.
- Oh, J.H., Kopp, G.A. and Incullet, D.R. (2007), "The UWO contribution to the NIST aerodynamic database for wind loads on low buildings. 3: Internal pressures", *J. Wind Eng. Ind. Aerod.*, **95**(8), 755-779.
- Sadek, F. and Simiu, E. (2002), "Peak non-Gaussian wind effects for database-assisted low-rise building design", *J. Eng. Mech.- ASCE*, **128**(5), 530-539.
- Sharma, R.N., Mason, S. and Driver, P. (2010), "Scaling methods for wind tunnel modelling of building internal pressures induced through openings", *Wind Struct.*, **13**(4), 363-374.
- Sharma R.N. and Richards P.J. (1997), "Computational modeling of the transient response of building internal pressure to a sudden opening", *J. Wind Eng. Ind. Aerod.*, **72**, 149-161.
- Sharma, R.N. and Richards, P.J. (2003), "The influence of Helmholtz resonance on internal pressures in a low-rise building", *J. Wind Eng. Ind. Aerod.*, **91**(6), 807-828.
- Sharma, R.N. and P.J. Richards, (1997), "The effect of roof flexibility on internal pressure fluctuations", *J. Wind Eng. Ind. Aerod.*, **72**(1-3), 175-186.
- Sharma, R.N. and Richards, P.J. (2005), "Net pressure on the roof of a low-rise building with wall openings", *J. Wind Eng. Ind. Aerod.*, **93**(4), 267-291.
- Sharma, R.N. (2000), "Transient response of building internal pressure to a sudden opening in the turbulent wind", *Proceedings of the 4th International Colloquium on Bluff Body Aerodynamics & Applications*, Bochum, Germany, September.
- Simiu, E. and Scanlan, R.H. (1996), *Wind Effects on Structures*, John Wiley and Sons.
- Simiu, E. and Stathopoulos, T. (1997), "Codification of wind loads on buildings using bluff body aerodynamics and climatological data bases", *J. Wind Eng. Ind. Aerod.*, **(69-71)**, 497-506.
- St.Pierre, L.M., Kopp, G.A., Surry, D. and Ho, T.C.E. (2005), "The UWO contribution to the NIST aerodynamic database for wind loads on low buildings. 2: Comparison of data with wind load provisions", *J. Wind Eng. Ind. Aerod.*, **93**(1), 31-59.
- Stathopoulos, T. and Luchian, H.D. (1989), "Transient Wind-Induced Internal Pressures", *J. Eng. Mech.- ASCE*, **115**(7), 1501-1514.
- Stathopoulos, T., Surry, D. and Davenport, A.G. (1979), "Internal pressure characteristics of low-rise buildings due to wind action", *Proceedings of the 5th International Conference on Wind Engineering*, Fort Collins, Colorado, Pergamon Press, New York, July.
- Teclé, A., Bitsuamlak, G. and Chowdhury, A. (2012), "Opening & Compartmentalization Effects of Internal Pressure in Low-Rise Buildings with Gable & Hip Roofs", *J. Archit. Eng.* (in press).
- Vickery, B.J. and Bloxham, C. (1992), "Internal pressure dynamics with a dominant opening", *J. Wind Eng. Ind. Aerod.*, **41**(1-3), 193-204.
- Vickery, B.J. (1986), "Gust factors for internal pressures in a low rise buildings", *J. Wind Eng. Ind. Aerod.*, **23**, 259-271.
- Vickery, B.J. and Bloxham, C. (1992), "Internal pressure dynamics with a dominant opening", *Proceedings of the 8th International Conference on Wind Engineering*, London, Ontario, Canada, July.
- Whalen, T., Simiu, E., Harris, G., Lin, J. and Surry, D. (1998), "The use of aerodynamic databases for the effective estimation of wind effects in main wind-force resisting systems: application to low buildings", *J. Wind Eng. Ind. Aerod.*, **(77-78)**, 685-693.
- Yeatts, B.B. and Mehta, K.C. (1992), "Field experiments for building aerodynamics", *Proceedings of the 2nd International Colloquium on Bluff Body Aerodynamics & Applications*, Melbourne, Australia, December.